



## Modeling graphene growth in the arc-discharge

Aichata Kane<sup>1,2</sup>, Ivaylo Hinkov<sup>3</sup>, Salim Mourad Chérif<sup>1</sup>, Aliou Hamady Barry<sup>2</sup>, Samir Farhat<sup>1</sup>

<sup>1</sup> Université Sorbonne Paris Nord, Laboratoire des Sciences des Procédés et des Matériaux, CNRS, LSPM-UPR 3407, F-93430, Villetaneuse, France

<sup>2</sup> Département de Chimie, Faculté des Sciences et Techniques de l'Université de Nouakchott AL-Assriya, Mauritanie

<sup>3</sup> Department of Chemical Engineering, University of Chemical Technology and Metallurgy, 8 Boulevard St. Kliment Ohridski, 1756 Sofia, Bulgaria

### Infos

Received: 15 February 2022

Accepted: 09 August 2022

### Keywords - Mots clés

modeling, graphene, arc discharge, synthesis, plasma

modélisation, graphène, arc électrique, synthèse, plasma

### Corresponding authors emails:

aita.kane6@gmail.com

### Abstract - Résumé

In this paper, 2D-axisymmetric steady state simulations was performed using computational fluid dynamics (CFD) code ANSYS FLUENT to simulate graphene growth under specific carbon arc discharge in helium atmosphere. Our arc model comprised the gas phase model coupled to the models of heat transfer, gas flow and carbon transport in the whole chamber, including the inter electrode region and the chamber bulk.

Dans cet article, des simulations en régime permanent axisymétrique 2D ont été réalisées à l'aide du code de dynamique des fluides ANSYS FLUENT afin de simuler la croissance du graphène sous une décharge d'arc dans une atmosphère d'hélium. Notre modèle tient compte de la chimie en phase gazeuse couplée aux modèles de transfert de chaleur, de flux des gaz et de transport du carbone dans l'ensemble de la chambre, y compris la région inter-électrode et le volume de la chambre.

## 1. INTRODUCTION

Since its isolation by Geim's team, research on graphene has exploded. This one-atom thick layer exhibit mechanical, optical and electrical interesting properties [1]. In 2009, Subrahmanyam *et al.* [2] have reported for the first time the synthesis of graphene flakes through the arc-discharge method. They used a graphite anode rod with different H<sub>2</sub>-He mixtures to produce graphene flakes with 2 – 4 layers in the inner wall region of the arc chamber. Karmakar *et al.* [3] demonstrate that graphene parameters can be controlled by an external steady non-uniform magnetic field. They succeeded in bulk synthesis of few-layer graphene by sublimating the graphite anode in an argon atmosphere. The magnetic field, enhance stacking of carbon precursors preferably along the surface of the cathode, assisting in the formation of graphene-sheet-like structures. As discussed by Moravsky *et al.* [4], externally applied magnetic field can deflect the flow of positively charged particles to enhance arc discharge process. In graphene context, the uncompensated positive charges that contribute to the cathode deposit could be limited to improve the graphene yield. Keidar *et al.* [5] discussed several approaches to improve the controllability of the arc discharge process for graphene and carbon nanotubes synthesis. This includes experimental improvements of the arc by applying external magnetic field as well as by proposing deterministic approaches to estimate from multispecies simulations electron density and temperature distribution. Vekselman *et al.* [6] performed comprehensive measurements of spatial and temporal profiles of carbon dimers (C<sub>2</sub>) in sub-atmospheric-pressure carbon arc by laser-induced fluorescence. They found that the measured spatial profiles of C<sub>2</sub> coincide with the growth region of carbon nanotubes and vary depending on the arc operation mode, which is determined by the discharge current and the ablation rate of the graphite anode. The comparison of their experimental data

with the 2D simulation results of self-consistent arc modeling showed good agreement. Yatom *et al* [7] studied the region of nanoparticle growth in an atmospheric pressure carbon arc. They used Two-dimensional computational fluid dynamic simulations of the arc combined with thermodynamic modeling, the simulation results completed by measurements of the planar laser-induced incandescence technique revealed presence large clouds of nanoparticles in the arc periphery bordering the region with a high density of  $C_2$  molecules. which is due to the interplay of the condensation of carbon molecular species and the convection flow pattern their results show that the nanoparticles are formed in the colder, peripheral regions of the arc and describe the parameters necessary for coagulation. Kane *et al.* [8] reported on a modified arc process to synthesize graphene, copper and zinc oxide graphene hybrids. Distinguishing features of such arcs are typically short length of about 3 mm inter-electrode gap and extremely hot ablating anode (4000 K) and plasma (10,000 K), which provides feedstock material for the growth of graphene. Numerical 2D-axisymmetric steady state simulations of the carbon arc discharge in helium atmosphere were performed using computational fluid dynamics (CFD) code ANSYS. The arc model comprised the gas phase model coupled to the models of heat transfer and electric current in the electrodes were solved to determine the velocity, temperature and chemical species distributions in the arc plasma under specific graphene synthesis conditions, thereby providing insight into growth mechanisms. The proposed model aimed to understand how the species behaves upon vaporization from the anode down to the cool regions of the reactor. Nevertheless, the model was limited to  $C_{11}$ , whereas, this is much fewer than the actual graphene sheet stoichiometry estimated at  $C_{16,400}$ . The organization of this article is as follow: in section 2 modeling which is divided into 3 parts: Model Equations, Boundary conditions, Solution strategy, results and discussion are presented in section 3 and conclusion in section 4.

## 2. MODELING

### 2.1. Model Equations

The arc vaporizes graphite anode in a background gas of helium. This vapor flowing from a sufficiently narrow arc gap can be idealized as a turbulent jet subjected to chemical reactions as well as heat and mass transfer in the reactor chamber [4]. These transfer phenomena control the dynamics of carbon vapor mixing with helium gas and the resulting cooling. In order to estimate the temperature profiles and species distribution in the plasma arc reactor under our typical conditions of graphene synthesis, a two-dimensional CFD modeling was performed by the commercial software ANSYS Fluent (version 15.0) [9]. Thermochemical and transport properties of the gas species as a function of temperature have been taken from Chemkin thermodynamic database [10–12] and NASA Reference publication [13]. The model uses the finite volume method to solve the governing equations, i.e., conservation of total mass, momentum and energy, and the individual species conservation equations. The 2-D axisymmetric computational domain, presented in Figure 1 was restricted to a limited part of the reactor including the plasma zone. The chosen

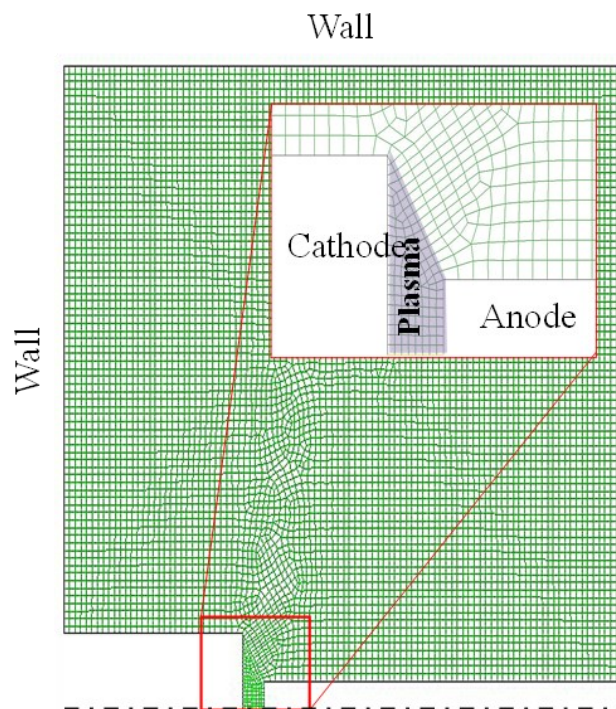


**Figure 1.** Computational domain and grid with a zoom of the gap region.

dimensions referred to the experimental setup. The distance between the anode and the cathode was fixed at 3 mm. The geometry was created using ANSYS Design Modeler and the mesh was generated using ANSYS Meshing application. The grid was composed of an unstructured quadrilateral mesh. The total number of cells was 8166 leading to a final grid with 7975 nodes, an average grid skewness of 0.2 and an orthogonal quality of 0.998. The very fine grid of the plasma zone was chosen to compute correctly the gradients of all transport variables between the two electrodes.

## 2.2. Boundary conditions

For initial and boundary conditions, the inlet was specified as a uniform inflow with axial velocity estimated on the basis of the measured anode erosion rate. The inlet temperature at the anode was fixed at 4000 K – the temperature of vaporization of the graphite. The water-cooled reactor walls, the anode and the cathode were modeled as wall boundary conditions at a constant temperature of 600 K for the reactor walls and 1000 K for the electrodes. The plasma heat was generated by constant volumetric source dependent on the input power and the plasma volume. The power density was homogeneously distributed inside the active plasma zone showed in figure 2. The radiative losses were neglected. The total pressure was fixed at 530 mbar. Turbulence was modelled using the k- $\epsilon$  turbulence approach. The Simple method for pressure-velocity coupling was selected. Simulations were carried out for two different current intensities, 120 A and 150 A.

## 2.3. Solution strategy

The model was developed based on the following assumptions:

- (i) The plasma was modeled using a steady state formulation. This assumption is justified by the continuous adjustment of the interelectrode gap, leading to a constant anode erosion rate.
- (ii) The plasma is assumed in local thermodynamic equilibrium (LTE). This hypothesis was based on the model of Bilodeau et al. [14] for fullerene synthesis by arc discharge in the same range of pressure as the graphene synthesis. Indeed, the arc plasma deviates from carbon LTE, but the abundance of carbon species in the arc region increases the collision frequency of carbons. This increases the electrical conductivity of the gas and reduces deviations from LTE.

For the simulation of the graphene condition, eleven neutral carbon species (from atomic carbon C to the cluster C11) were involved in the gas-phase chemistry. The ions and electrons were not considered. This assumption affected the accuracy of the calculations. However, an effort was made here to only estimate the plasma temperature and major gas species concentrations. The considered gas-phase reversible reactions between the carbon species and rate coefficients are given in Table 1 from Krestinin et al. [15].

Helium (He) was used as inert gas and we assumed a dilution factor of  $\tau = 20$ . This factor accounts for the mixing of carbon coming from the anode erosion with the inert atmosphere. It is defined by the ratio:

$$\tau = \frac{\text{moles (Carbon)}}{\text{moles (Carbon + He)}} \quad 1$$

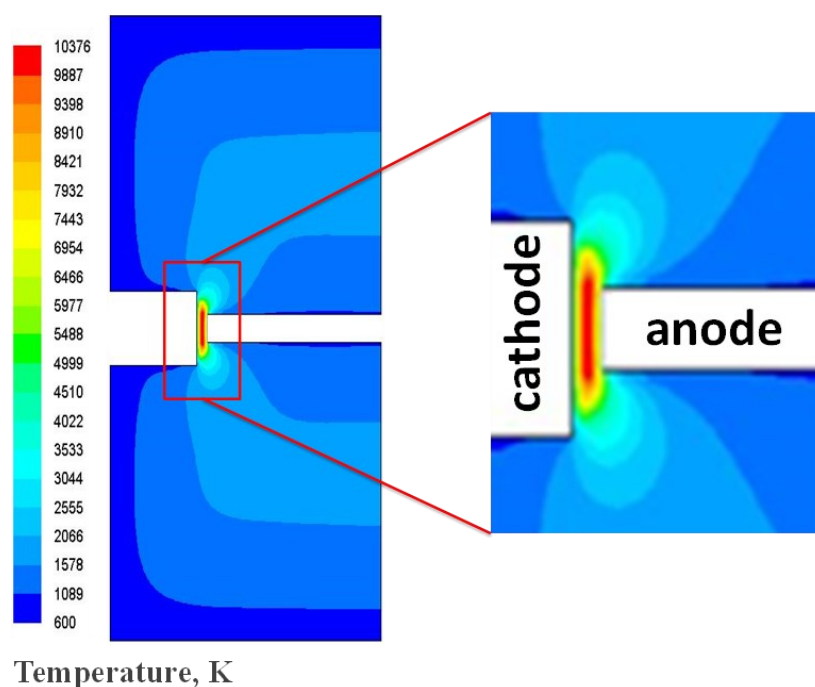


**Figure 2.** Homogeneously distribution of the power density inside the active plasma zone

**Table 1.** Gas phase chemistry used for graphene simulation

Gas Phase Reactions <sup>1</sup>	A (cm <sup>3</sup> /s/mol)	$\beta$ (-)	E (K)
C + C = C <sub>2</sub>	2×10 <sup>14</sup>	0	0
C + C <sub>2</sub> = C <sub>3</sub>	2×10 <sup>14</sup>	0	0
C <sub>2</sub> + C <sub>2</sub> = C <sub>3</sub> + C	2×10 <sup>15</sup>	0	9040
C <sub>2</sub> + C <sub>2</sub> = C <sub>4</sub>	2×10 <sup>14</sup>	0	0
C + C <sub>3</sub> = C <sub>4</sub>	2×10 <sup>14</sup>	0	0
C + C <sub>4</sub> = C <sub>5</sub>	2×10 <sup>14</sup>	0	0
C <sub>2</sub> + C <sub>3</sub> = C <sub>5</sub>	2×10 <sup>14</sup>	0	0
C <sub>5</sub> + C = C <sub>6</sub>	2×10 <sup>14</sup>	0	0
C <sub>6</sub> + C = C <sub>7</sub>	2×10 <sup>14</sup>	0	0
C <sub>7</sub> + C = C <sub>8</sub>	2×10 <sup>14</sup>	0	0
C <sub>8</sub> + C = C <sub>9</sub>	2×10 <sup>14</sup>	0	0
C <sub>9</sub> + C = C <sub>10</sub>	2×10 <sup>14</sup>	0	0
C <sub>4</sub> + C <sub>2</sub> = C <sub>6</sub>	2×10 <sup>14</sup>	0	0
C <sub>5</sub> + C <sub>2</sub> = C <sub>7</sub>	2×10 <sup>14</sup>	0	0
C <sub>6</sub> + C <sub>2</sub> = C <sub>8</sub>	2×10 <sup>14</sup>	0	0
C <sub>7</sub> + C <sub>2</sub> = C <sub>9</sub>	2×10 <sup>14</sup>	0	0
C <sub>8</sub> + C <sub>2</sub> = C <sub>10</sub>	2×10 <sup>14</sup>	0	0
C <sub>9</sub> + C <sub>2</sub> = C <sub>11</sub>	2×10 <sup>14</sup>	0	0
C <sub>3</sub> + C <sub>3</sub> = C <sub>6</sub>	2×10 <sup>14</sup>	0	0
C <sub>4</sub> + C <sub>3</sub> = C <sub>7</sub>	2×10 <sup>14</sup>	0	0
C <sub>5</sub> + C <sub>3</sub> = C <sub>8</sub>	2×10 <sup>14</sup>	0	0
C <sub>6</sub> + C <sub>3</sub> = C <sub>9</sub>	2×10 <sup>14</sup>	0	0
C <sub>7</sub> + C <sub>3</sub> = C <sub>10</sub>	2×10 <sup>14</sup>	0	0
C <sub>4</sub> + C <sub>4</sub> = C <sub>8</sub>	2×10 <sup>14</sup>	0	0
C <sub>5</sub> + C <sub>4</sub> = C <sub>9</sub>	2×10 <sup>14</sup>	0	0
C <sub>6</sub> + C <sub>4</sub> = C <sub>10</sub>	2×10 <sup>14</sup>	0	0
C <sub>5</sub> + C <sub>5</sub> = C <sub>10</sub>	2×10 <sup>14</sup>	0	0

<sup>1</sup> Forward rate constants  $k$  are calculated assuming Arrhenius temperature dependence  $k = A \times T^\beta \times \exp(-E/RT)$  where  $A$  is the pre-exponential factor,  $\beta$  is the temperature exponent and  $E$  is the activation energy.

### 3. RESULTS AND DISCUSSION

The purpose to resolving this model is to predict the distribution of the species and temperature in arc reactor under our synthesis conditions. Figure 3 (a-c) shows the experimental set-up used to synthesis graphene and hybrids GrCu and GrZnO. The experimental results shows graphene sheets for Gr samples and carbon shells capping the copper core for GrCu (Figure 3d, 3e), also a Raman spectra (Figure 3f) which certifies that the graphene sheets are of good structural quality[4].

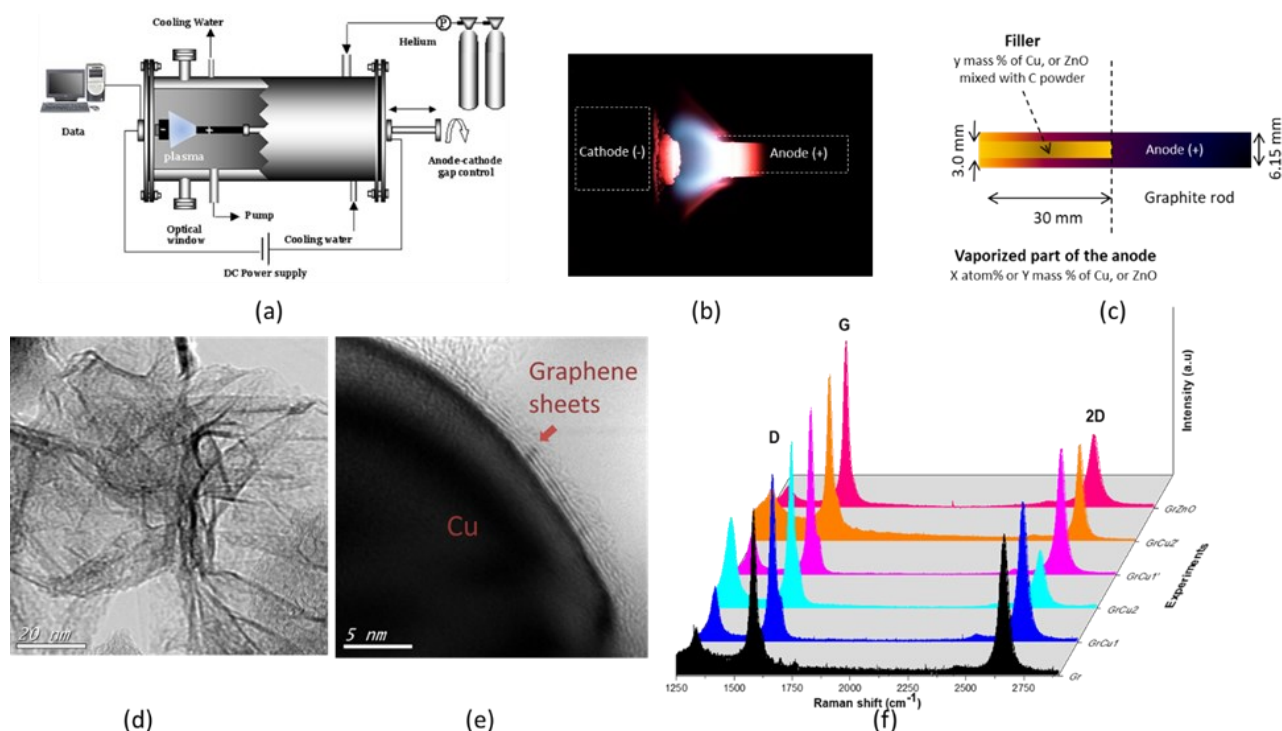


**Figure 3.** LSPM's Arc discharge set-up. (a) schematic; (b) photograph of the luminous plasma zone created between the anode and the cathode and (c) anode composition; (d) Graphene HRTEM (scale 20 nm); (e) Gr-Cu hybrids HRTEM (scale 5 nm); Raman of graphene and GrCu and GrZnO hybrids. After [8].

For the species distribution in the reactor, the simulated molar fraction profiles of small carbon clusters  $C-C_3$  and higher mass carbon clusters  $C_9-C_{11}$  at 150 A are presented in Figure 4. This Figure shows that atomic C was the major carbon specie in the plasma. Other species such as  $C_2$  and  $C_3$  had also a rather important contribution to the graphene synthesis. They were formed on the front face of the cathode as well as in the region close to the plasma.

Higher mass carbon clusters such as  $C_9$ ,  $C_{10}$  and  $C_{11}$  were relegated to the cold walls of the reactor (see Figure 4) where graphene was expected to form. Similar profiles were also found for a current of 120 A. The 2-D calculated temperature contours of arc discharge plasma and 1-D temperature profiles along the centerline of plasma in the interelectrode gap are shown in Figure 5.

It can be seen that the maximal temperature in the center of the plasma reaches 9200 K at 120 A and 10,400 K at 150 A. These values are in the same order of magnitude of measurements of the optical emission spectra obtained in our setup for various combinations of gap width, position in the gap, radius, arc current and gas pressure. The thermal balance of plasma heating and cathode cooling determines the cathode temperature. Hence, there is a steep temperature gradient between the cathode and the region where the temperature is the highest. The flow and trajectories of gas species are visualized on Figure 5a by using the velocity path lines. The maximum velocity is 4 m/s, which is sufficient to ensure a fully turbulent jet in the narrow arc gap, as was shown on the picture made by Hinkov and Farhat (Figure 5b [16]). The presence of vortices around the electrodes is supposed to control the dynamics of carbon vapor mixing with helium gas and the resulting cooling thereby increasing the mass flux gas species from the plasma zone to the cold cathode region.

In Figure 7, LSPM's plasma model was benchmarked with Princeton's group simulations [Khrabry *et al.*, 2019]. The presence of vortices around the electrodes controlled the dynamics of carbon vapor mixing with helium gas thereby increasing the mass flux gas species from the plasma zone to the cold cathode region. Small carbon clusters, e.g.,  $C_2$  are envisioned to form higher carbonaceous species that would tend to grow fragments of graphene. Since complete fluid dynamics in three dimensions wider models presents a formidable computational task, it may be possible to improve this chemical modeling by lumping many clusters into a representative clusters  $C_n$  and consider their interaction with small carbon fragments  $C_m$  ( $m = 1, 2, \dots$ ) via reactions  $C_n + C_m \rightarrow Gr$  [8].

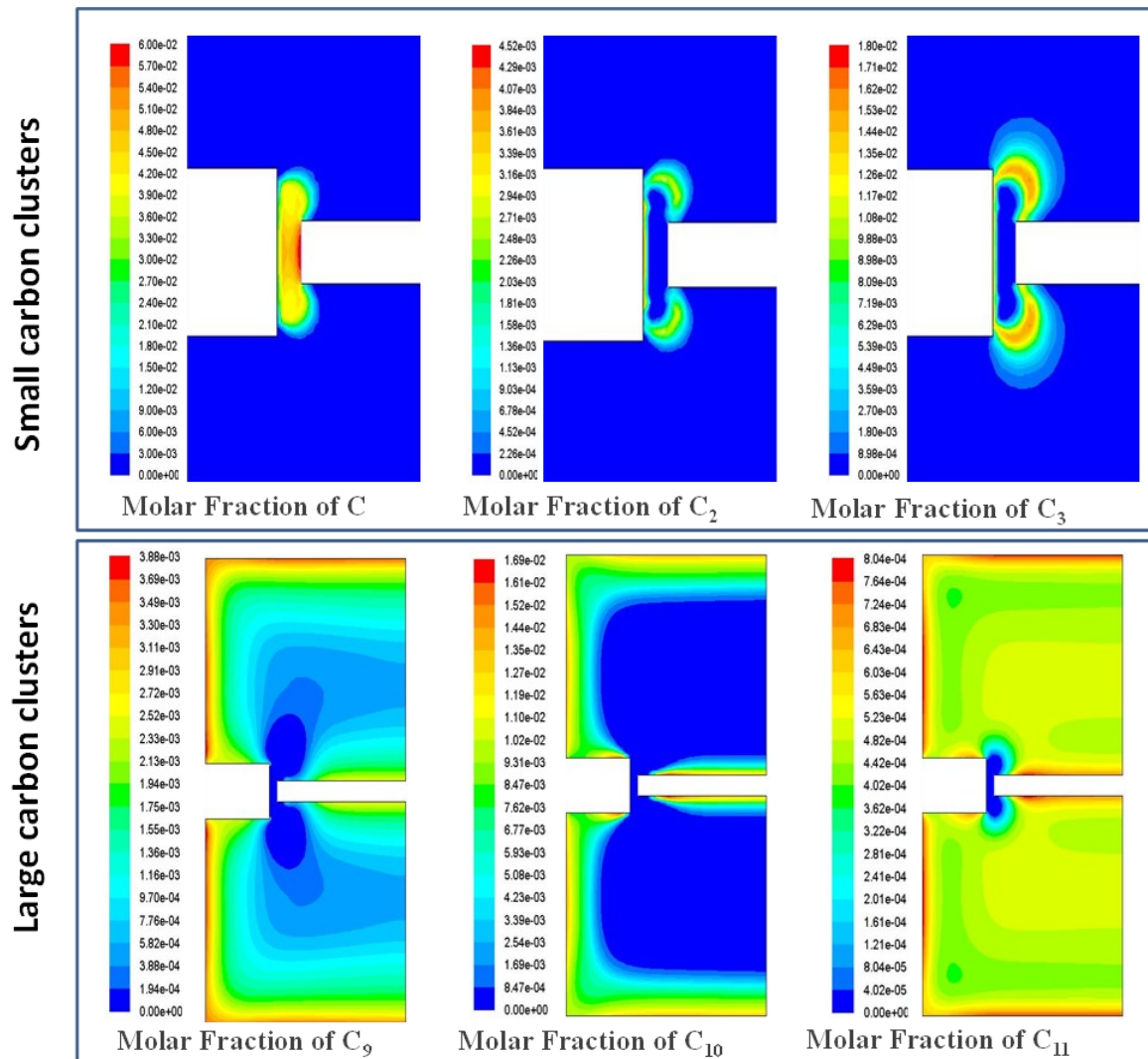


Figure 4. Simulated mole fractions of small carbon clusters C–C<sub>3</sub> and higher mass carbon cluster C<sub>9</sub>–C<sub>11</sub> at 150 A.

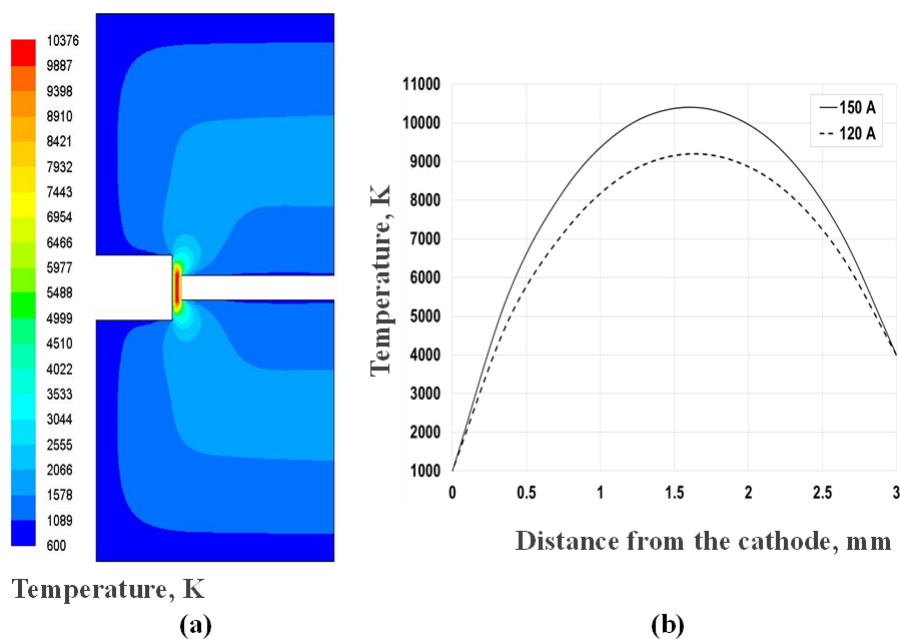
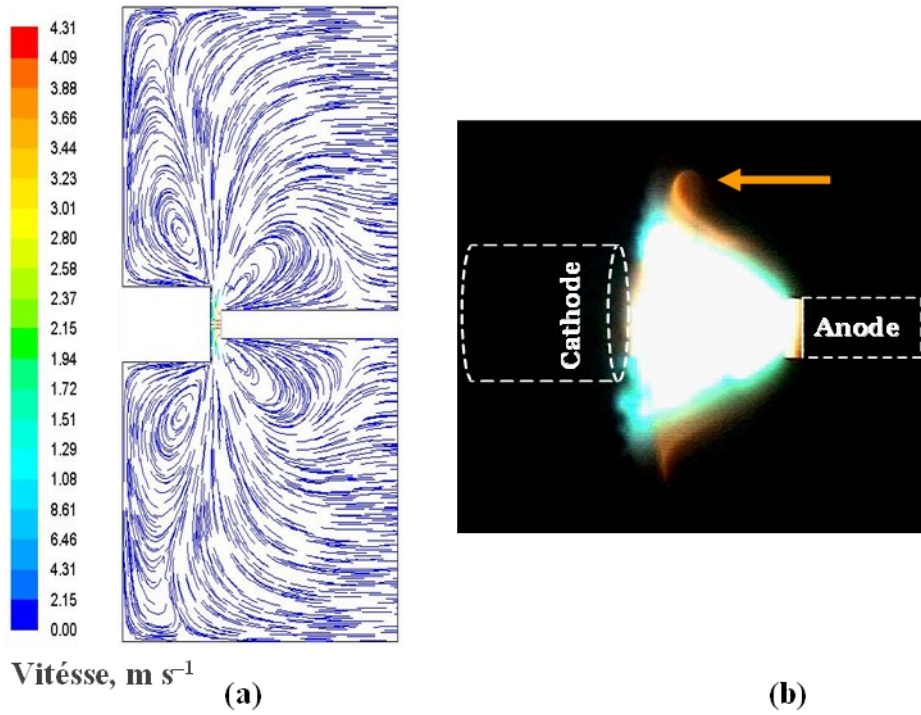
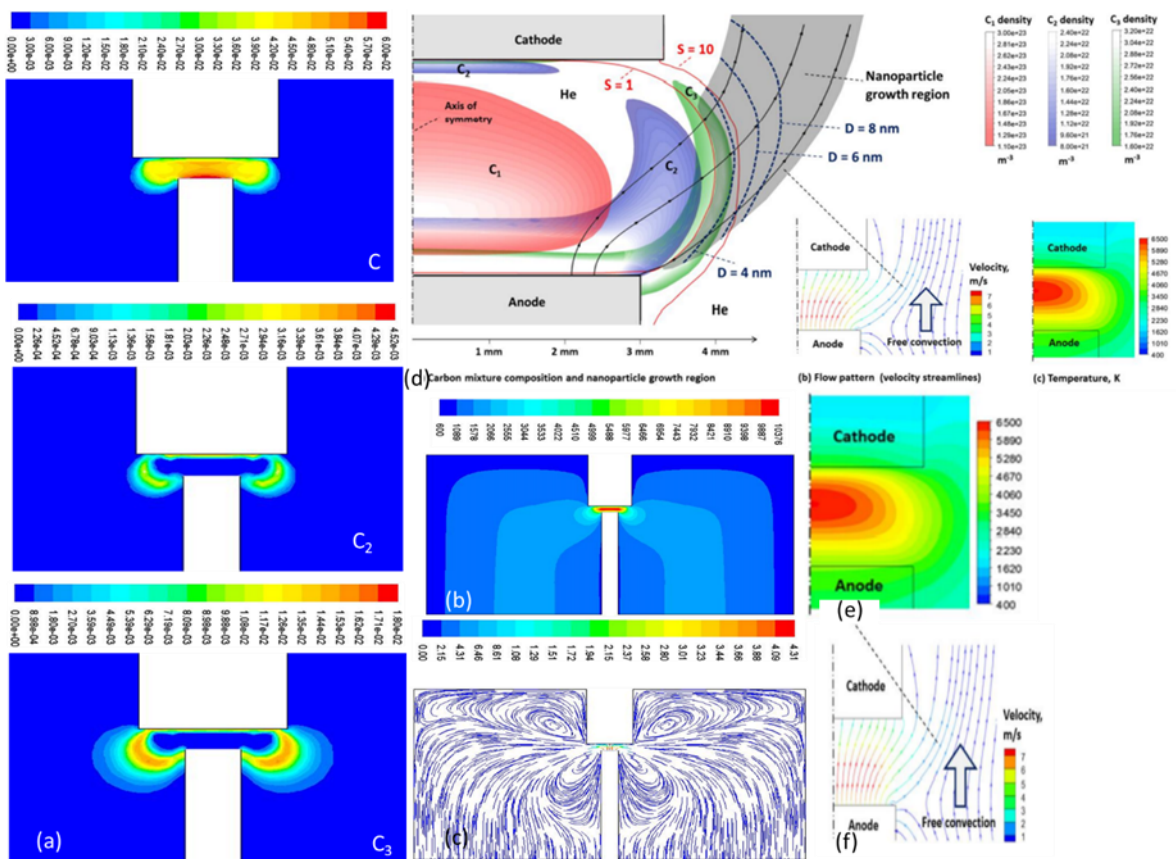


Figure 5. (a) Simulated temperature distribution inside the reactor at 150 A, (b) onedimensional (1D) temperature profiles along the centerline between the anode and the cathode at 120 A (dashed line) and 150 A (continuous line).



**Figure 6.** (a) Calculated velocity path lines in the reactor at 150, (b) plasma image showing a turbulent jet in the inter-electrode space. After [16]



**Figure 7.** Results of the carbon arc simulations for graphene synthesis. LSPM (a-c) vs Princeton (d-f). (a and d) Density profiles of various carbon species along flow streamlines; (b and e) gas temperature profile; (c and f) flow pattern. After [8] and [17]

#### 4. CONCLUSIONS

Our modeling gave a better understanding of the behavior of the species distribution. It is especially important to understand how the species behaves upon vaporization from the anode down to the cool regions of the reactor. We limited the carbon atoms in the model to  $C_{11}$ , whereas, There are hundreds of species possible, ranging from atomic carbon to large clusters of carbonaceous soot  $C_n$ . In the case of a circular graphene sheet of 124 nm diameter as found in our experiments, their surface area is  $12,000 \text{ nm}^2$ . Considering the C–C bond length of  $d = 1.421 \text{ \AA}$ , the area of an individual hexagon of the honeycomb is  $3/2\sqrt{3}d^2$  namely  $0.369 \text{ nm}^2$ . Since each hexagon in the lattice contains 2 full atoms (6 atoms with a third of each inside the hexagon), the monolayer graphene sheets will have a stoichiometry  $C_{16,400}$ . Due to the significant computer time required for models containing large numbers of species used in computational fluid dynamic (CFD) simulations, large models are impractical for simulating. The calculated flow and trajectories attested a fully turbulent jet in the narrow arc gap. The presence of vortices around the electrodes controlled the dynamics of carbon vapor mixing with helium gas thereby increasing the mass flux gas species from the plasma zone to the cold cathode region. Small carbon clusters, e.g.,  $C_2$  are envisioned to form higher carbonaceous species that would tend to grow fragments of graphene. Since complete fluid dynamics in three dimensions plus large models presents a formidable computational task, it may be possible to improve the actual chemical modelling by lumping many clusters into a representative clusters  $C_n$  and consider their interaction with small carbon fragments  $C_m$  ( $m = 1,2,\dots$ ) via reactions  $C_n + C_m \rightarrow \text{Gr}$ .

#### ACKNOWLEDGMENTS

ANR (Agence Nationale de la Recherche), and CGI (Commissariat à l'Investissement d'Avenir) are gratefully acknowledged for their financial support of this work through Labex SEAM (Science and Engineering for Advanced Materials and devices) ANR 11 LABX 086, ANR 11 IDEX 05 02, and ANR-14CE08-0018. Embassy of France in Nouakchott, Mauritania and University of Nouakchott AL-Assriya are gratefully acknowledged for funding through international mobility fellowship.

#### REFERENCES

- [1] K.S. Novoselov, A.K. Geim, S.V. Morozov, D. Jiang, Y. Zhang, S.V. Dubonos, I.V. Grigorieva, A.A. Firsov, *Science*, 306 (2004) 666.
- [2] K. S. Subrahmanyam, L. S. Panchakarla, A. Govindaraj and C. N. R. Rao, *J. Phys. Chem. C.*, 113 (2009) 4257.
- [3] S Karmakar, N. V Kulkarni, A. B Nawale, N. P Lalla, R. Mishra, V G Sathe, S V Bhoraskar, A K Das, *J. Phys. D: Appl. Phys.*, 42 (2009) 115201.
- [4] A.P Moravsky, E. M. Wexler, R. O. Loutfy, *Growth of carbon nanotubes by arc discharge and laser ablation. In Carbon Nanotubes Science and Applications*; pp. 65–97, Meyyappan, M., Ed.; CRC Press: Boca Raton, FL, USA, 2004.
- [5] M. Keidar, A. Shashurin, J. Li, O. Volotskova, M. Kundrapu, T.S. Zhuang, *J. Phys. D Appl. Phys.*, 44 (2011) 174006.
- [6] V. Vekselman, A. Khrabry, I. Kaganovich, B. Stratton, R. S. Selinsky, Y. Raitses, *Plasma Sources Sci. Technol.*, 27 (2018) 025008.
- [7] S. Yatom, A. Khrabry, J. Mitran, A. Khodak, I. Kaganovich, V. Vekselman, B. Stratton, Y. Raitses, *MRS Communications*, (2018), 1 of 8
- [8] A. Kane, I. Hinkov, O. Brinza, M. Hosni, A. H. Barry, S.M. Cherif, S. Farhat, *coatings*, 10 (2020) 308.
- [9] ANSYS Fluent User's Guide, Release 15.0; ANSYS, Inc.: Canonsburg, PA, USA, 2013.
- [10] R. J. Kee, F. M. Rupley, J. A. Miller, M. E. Coltrin, J. F. Grear, E. Meeks, H. K. Moat, A. E. Lutz, G. D Lewis, M. D. Smooke, et al. CHEMKIN Collection, Release 3.6; Reaction Design, Inc.: San Diego, CA, USA, 2001.
- [11] JANAF. Report NSRDS-NBS: Dow Chemical Company, Clearinghouse for Federal Scientific and Technical Information; PB168370; Springfield: Virginia, VA, USA, 1965.
- [12] R.J Kee, G.D Lewis, J. Warnatz, J. A. Miller, *Technical Report SAND86-8426; Sandia National Laboratories: Albuquerque, NM, USA, 1986.*
- [13] R. Gupta, J. Yos, R. Thompson, K. A. Lee, *NASARP-1232; NASA Reference Publication: Hampton, VA, USA, 1990.*
- [14] J.F Bilodeau, J. Pousse, A. A. Gleizes, *Plasma Chem. Plasma Process.*, 18 (1998).
- [15] A.V. Krestinin, A.P. Moravskii, P.A. Tesner, *Chem. Phys. Rep.*, 17((1998).
- [16] I. Hinkov and S. Farhat, Proceedings of the 6th NASA/CP-2001.
- [17] A. Khrabry, I.D. Kaganovich, A. Khodak, V. Vekselman, Y. Raitses. ISPC24 –24th International Symposium on Plasma Chemistry, Naples (Italy) June 9-14, 2019.